ELSEVIER

Scopus

doi

Journal of Vibration Engineering

ISSN:1004-4523

Registered

- SCOPUS
- GOOGLE SCHOLAR
- DIGITAL OBJECT IDENTIFIER (DOI)
- IMPACT FACTOR 6.1

Our Website
www.jove.science

TAGUCHI'S OPTIMIZATION OF FUSED DEPOSITION MODELING FOR 3D PRINTED CARBON FIBER REINFORCED PLA- PRO COMPOSITE: THE IMPACT OF PRINTING PARAMETERS

AVIRNENI KRISHNA CHAITANYA[1], LAKSHMI PRASAD[2], R. NAGENDRA BABU[3]

[1]M.Tech Student, Department Of Mechanical Engineering, Sree Vahini Institute Of Science & Technology, Tiruvuru-521 235, AP, India.

[2]Assistant Professor, Department Of Mechanical Engineering, Sree Vahini Institute Of Science & Technology, Tiruvuru-521 235, AP, India.

[3]Professor, Department Of Mechanical Engineering, Sree Vahini Institute Of Science & Technology, Tiruvuru-521 235, AP, India.

Abstract

Fused Deposition Modelling (FDM) has emerged as an effective additive manufacturing technique for fabricating polymer and polymer-matrix composites reinforced with various materials. In this study, chopped short carbon fibers were incorporated into polylactic acid pro (PLA PRO) to enhance its mechanical performance, targeting a 30% improvement in overall strength. The composite specimens were fabricated using FDM and evaluated for their tensile strength, flexural strength, and Izod impact strength. Taguchi's optimization method was employed to determine the optimal combination of printing parameters that maximize these mechanical properties. The influence of key process parameters layer height, printing orientation, extrusion temperature, air gap, and nozzle material was systematically investigated. Results revealed that the careful optimization of these parameters led to substantial improvements in performance. The addition of short carbon fibers (8μm in length and 300μm in diameter) significantly enhanced the tensile strength (61 MPa), flexural strength (70 MPa), and Izod impact strength (480 J/m) of the composite, corresponding to an approximate 30-40% increase compared with pure PLA. Among the investigated parameters, layer height and nozzle material were identified as the most influential factors affecting the mechanical behavior of carbon fiber-reinforced PLA composites.

Keywords: PLA (polylactic acid) · Carbon fiber, FDM (fused deposition modelling), Taguchi's optimization, Mechanical characterization.

1. Introduction

Additive Manufacturing (AM), commonly known as 3D printing, is an advanced fabrication technique that transforms virtual three-dimensional models developed through Computer-Aided Design (CAD) or scanning into tangible objects by sequentially depositing material layers. Unlike traditional subtractive or formative manufacturing methods, AM eliminates the need for labour-intensive mold preparation or machining, thereby enabling direct fabrication in a single process step [1]. To overcome the limitations of conventional manufacturing, AM has been increasingly employed in the development of polymer composites, enabling the effective integration of matrix and reinforcement materials. This combination results in composite systems exhibiting superior structural and functional characteristics compared to the individual constituents [2]. Reinforcing polymers with particles, natural or synthetic fibers, or nanomaterials can significantly enhance their mechanical performance and broaden their functional utility [3]. Traditional composite manufacturing methods such as moulding, casting, and machining often encounter challenges when producing components with complex geometries [4]. In contrast, 3D printing offers precise control over geometry and dimensions through CAD-driven fabrication, minimizing material waste while allowing the creation of intricate composite structures. This process flexibility, combined with enhanced performance, makes 3D-printed composites particularly attractive for engineering applications.

Recent research efforts have focused on developing advanced thermoplastic-based composites reinforced with fibers to improve mechanical strength and functionality. Common thermoplastic matrices include polypropylene (PP), thermoplastic polyurethane (TPU), polyester, and nylon, which are often reinforced with glass or carbon fibers of varying lengths. For instance, alkali-treated (5% NaOH) hemp fiber-reinforced polycarbonate composites containing 10 wt% fiber have demonstrated superior structural performance compared to unreinforced alternatives [5]. Furthermore, reinforcing polymers with sustainable and reusable materials such as short or long carbon fibers enhances their suitability for high-performance and environmentally conscious engineering applications [6,7]. Carbon fiber-reinforced polymer (CFRP) composites have gained significant attention in industrial fabrication owing to their exceptional mechanical strength, corrosion resistance, and lightweight nature. Carbon fiber-based additive manufacturing, in particular, addresses the inherent challenges of conventional polymer composites, such as material wastage and limited mechanical robustness [8]. As a result, components produced through this process exhibit properties comparable to,

or even exceeding, those of traditionally manufactured polymer matrix composites, making them highly desirable for modern industrial and structural applications.

Previous studies have demonstrated that the incorporation of carbon fibers into acrylonitrile butadiene styrene (ABS) significantly enhances its mechanical strength within a short processing period [9]. The mechanical behavior of carbon fiber-reinforced composites has also been evaluated using multi-axial testing machines, particularly for moving structural components. Similarly, the integration of carbon fibers into polyether ether ketone (PEEK)-based polymer composites has been shown to improve mechanical performance across various engineering applications while contributing to notable weight reduction in automotive structures [10]. Further research has investigated the influence of carbon fiber reinforcement on the mechanical characteristics of polylactic acid (PLA) composites, considering variations in fiber length and volume fraction. Taguchi's optimization method was employed to determine the optimal process parameters that enhance mechanical performance [11].

In accordance with ASTM standards, the tensile, flexural, and impact strengths of the 3D-printed specimens were experimentally evaluated. The primary objective of this study is to optimize key printing parameters such as nozzle material, layer height (LH), air gap (AG), printing orientation, and extrusion temperature to improve the mechanical properties of carbon fiber-reinforced PLA composites fabricated through Fused Deposition Modelling (FDM). The selected parameters included layer heights of 0.1, 0.2, and 0.3 mm; air gaps of 0.8, 0.53, and 0.4 mm corresponding to infill densities of 75%, 50%, and 100%, respectively; orientations of 0°, 45°, and 90°; and extrusion temperatures of 200°C, 210°C, and 220°C. Tensile and flexural specimens were fabricated using the FDM process and tested according to the corresponding ASTM standards to evaluate tensile strength (TS), flexural strength (FS), and Izod impact strength (IM). Recent literature highlights the growing significance of carbon fiber-reinforced polymer composites particularly PLA-based systems in additive manufacturing, owing to their potential for achieving superior strength-to-weight ratios and enhanced performance. Taguchi's optimization technique was further applied in this study to systematically analyze and improve the influence of printing parameters on the mechanical behavior of the carbon fiber-reinforced PLA composites.

Table 1: Material Used in FDM

Matrix	Reinforcement Material	Composition (Matrix & Reinforcement)
PLAPRO	Short Carbon Fiber ≈ 300µm length	80%,20%

Fig. 1 FDM printer

2 Materials and methods

2.1 3D Printing of composite specimen

In this investigation, a composite material consisting of polylactic acid (PLA PRO) reinforced with 20 wt% short carbon fibers was utilized. The carbon fibers were mechanically chopped to an average length of 300µm and a diameter of approximately 8µm, as summarized in Table 1. Specimen fabrication was carried out using the Fused Deposition Modelling (FDM) process on a customized RepRap 3D printer equipped with a build volume of 220 × 220 × 300 mm, as illustrated in Figure 1. The printer configuration and process settings were refined based on prior studies that investigated the influence of FDM process parameters on the printability and mechanical performance of polymer composites. The optimized printing parameters employed for the fabrication of test specimens used for mechanical characterization are presented in Table 2.

Table - 2: Printing parameters of FDM Machine setup

Parameter	Value	Unit
Air Gap/Infill density	0.4/100	Mm/%
Temperature	220	^{0}C
Layer Height	0.2	mm
Raster Angle orientation	90	^{0} Degree

2.2 Taguchi Model

The Taguchi method is a robust statistical optimization technique widely employed to enhance the quality and consistency of manufacturing processes by minimizing variability and identifying optimal parameter settings. When applied to Fused Deposition Modelling (FDM), this approach facilitates the production of high-performance printed components at lower cost through systematic process optimization. Taguchi's methodology utilizes orthogonal arrays to design experiments efficiently, allowing the simultaneous investigation of multiple process parameters with a minimal number of experimental runs. Unlike traditional full-factorial designs, which require exhaustive testing of all possible parameter combinations, the Taguchi approach significantly reduces experimental complexity while maintaining statistical validity in determining the influence of each factor on the output quality.

In this study, the L27 orthogonal array was adopted (as shown in Tables 3 and 4) to evaluate the effects of five key FDM process parameters layer height, air gap, orientation, nozzle material, and extrusion temperature on the mechanical performance of carbon fiber-reinforced PLA composites. To assess performance variability and optimize process robustness, the signal-to-noise (S/N) ratio was computed for each experimental condition. The "larger-the-better" criterion was applied to maximize desirable mechanical properties such as tensile strength, flexural strength, and impact resistance. The S/N ratio for this criterion is calculated using the following equation:

$$\eta = -10\, log_{10}\left[\left(\frac{1}{n}\right)\sum_{i=1}^{n}\frac{1}{y^2}\right] \qquad (1)$$

Where, n=Sample Size, and y=Objective function in that run.

This formulation ensures that higher performance values correspond to larger S/N ratios, indicating improved process stability and product quality. Through this optimization

framework, the Taguchi method effectively enhances the mechanical reliability, reproducibility, and cost-efficiency of FDM-processed carbon fiber-reinforced PLA- PRO composites.

2.3 Testing

Tensile, flexural, and impact test specimens were fabricated using the Fused Deposition Modelling (FDM) process in accordance with ASTM D638 and ASTM D790 standards, as illustrated in Figures 2 and 3 [10]. Mechanical testing was performed using a universal testing machine (Model: JINAN-100KN) equipped with a 5 kN load cell and operated at a crosshead speed of 2 mm/min for both tensile and flexural evaluations. The Izod impact strength was determined according to the ASTM D256 standard. In alignment with the L_{27} orthogonal array design, three replicate specimens were tested for each experimental condition to ensure result reliability and statistical consistency.

Microstructural characterization of the printed composites was carried out using an OLYMPUS GX3 digital optical microscope to analyze the dispersion of carbon fibers within the PLA-PRO matrix and to assess the quality of interfacial bonding between the fiber and the polymer. The composite specimens comprising PLA-PRO reinforced with short carbon fibers were evaluated for tensile strength, flexural strength, and Izod impact strength to determine the influence of printing parameters and reinforcement characteristics on mechanical performance. While prior studies have predominantly investigated the influence of varying fiber lengths on mechanical properties, the present research focuses on examining the effect of a 300μm carbon fiber length on the composite's mechanical response. The results obtained from these standardized experimental procedures and subsequent analyses provide valuable insights into the relationship between fiber reinforcement, FDM process parameters, and the resulting mechanical behavior of carbon fiber-reinforced PLA-PRO composites [12].

Table 3: Parameters set for the optimization through L_{27} array

Symbol	A	B	C	D	E
Levels	Layer Height (mm)	Air Gap (mm)	Orientation (Degree)	Temperature (°C)	Nozzle (Number)
1	0.2	0.6	0	210	BR-(1)
2	0.3	0.4	45	220	HS-(2)

3	0.4	0.3	90	230	TiC-(3)

Table 4: L_{27} orthogonal array for the process parameters

No.Exp	Layer height LH (mm)	Air gap AG (mm)	Orientation OR (Deg)	Temperature (°C)	Nozzle number
S1	0.2	0.6	0	210	1
S2	0.2	0.6	0	210	2
S3	0.2	0.6	0	210	3
S4	0.2	0.4	45	220	1
S5	0.2	0.4	45	220	2
S6	0.2	0.4	45	220	3
S7	0.2	0.3	90	230	1
S8	0.2	0.3	90	230	2
S9	0.2	0.3	90	230	3
S10	0.3	0.6	45	230	1
S11	0.3	0.6	45	230	2
S12	0.3	0.6	45	230	3
S13	0.3	0.4	90	210	1
S14	0.3	0.4	90	210	2
S15	0.3	0.4	90	210	3
S16	0.3	0.3	0	220	1
S17	0.3	0.3	0	220	2
S18	0.3	0.3	0	220	3
S19	0.4	0.6	90	220	1
S20	0.4	0.6	90	220	2
S21	0.4	0.6	90	220	3
S22	0.4	0.4	0	230	1
S23	0.4	0.4	0	230	2
S24	0.4	0.4	0	230	3
S25	0.4	0.3	45	210	1
S26	0.4	0.3	45	210	2
S27	0.4	0.3	45	210	3

$$Tensile\ Strength\ , \sigma = \frac{F}{A} \qquad (2)$$

$$Flexural\ Strength\ = \frac{3FL}{2bd^2} \qquad (4)$$

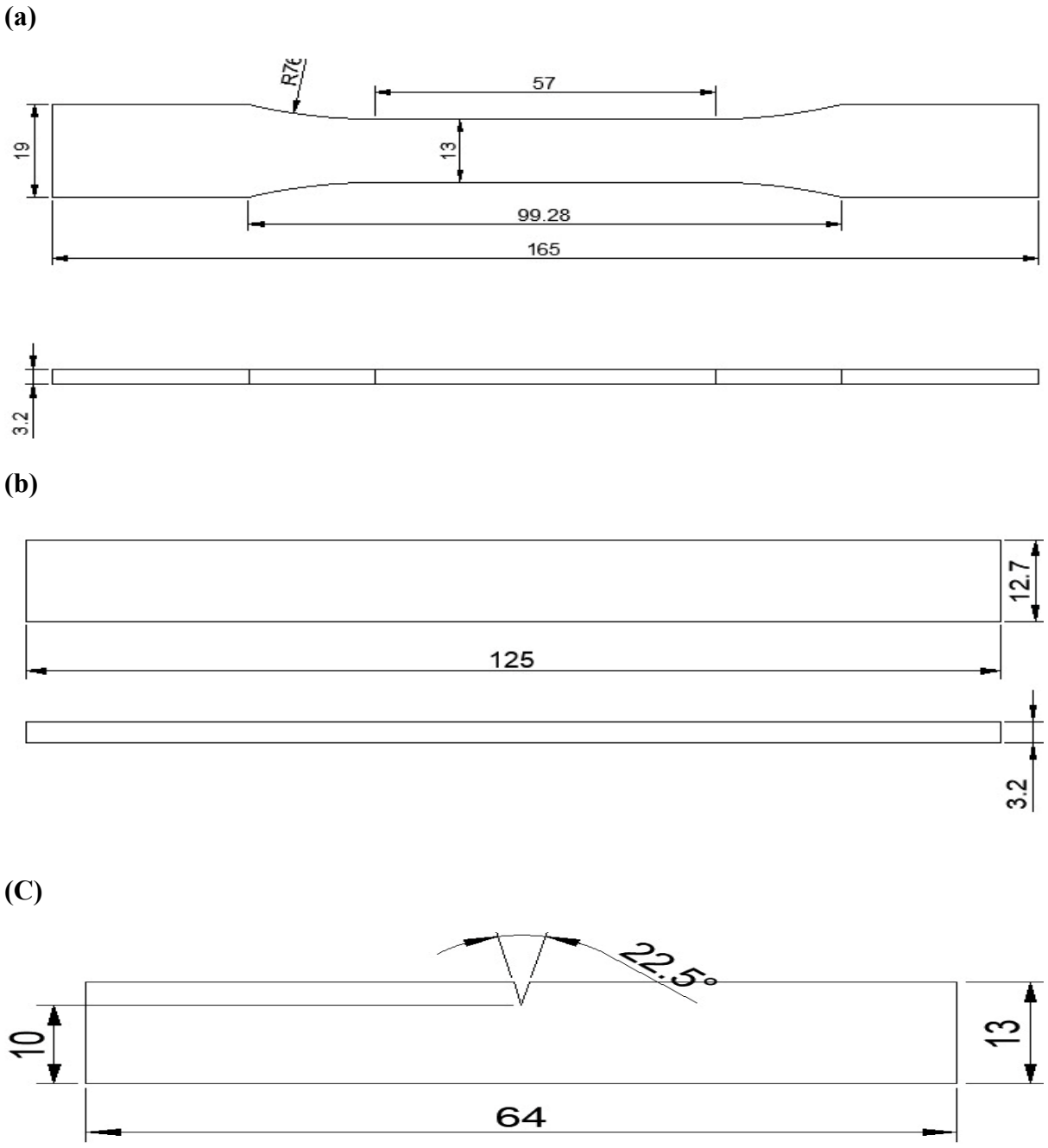

Figure 2: A) Tensile specimen (B)Flexural specimen (C) Impact specimen used for testing mechanical properties

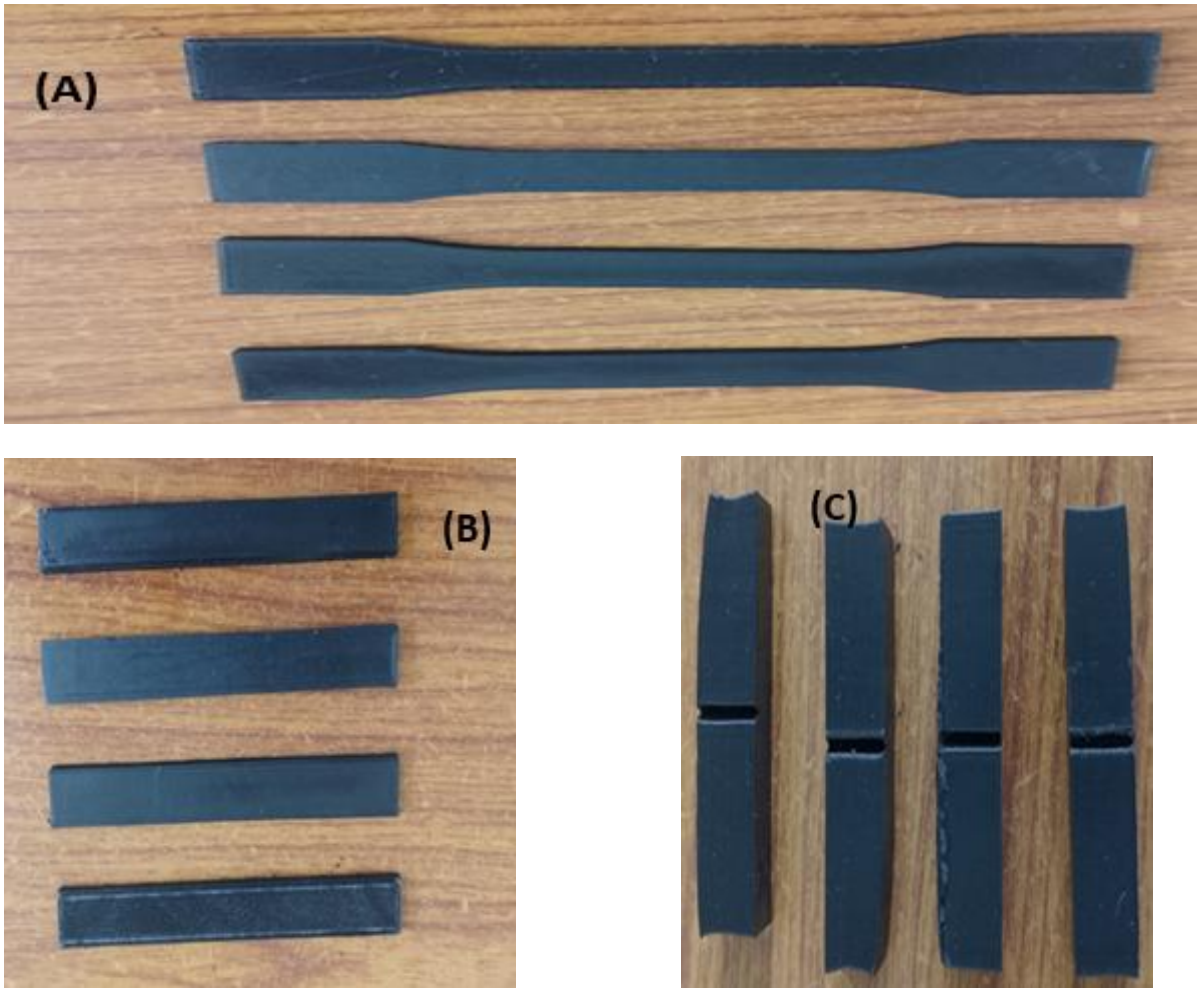

Fig: 3: 3D printed (A)Tensile, (B)Flexural, (C) Impact samples by C-PLA-PRO composite

3 Results and discussion

In accordance with ASTM testing standards, the 3D-printed specimens were evaluated for tensile strength (TS), flexural strength (FS), and impact strength (IM) under varying process conditions. The mean values of these mechanical properties, obtained from three independent tests conducted for each specimen, are presented in Figure 4-12. The experimental design was based on Taguchi's L_{27} orthogonal array, and the corresponding signal-to-noise (S/N) ratios for all mechanical parameters are summarized in Table 5-22.

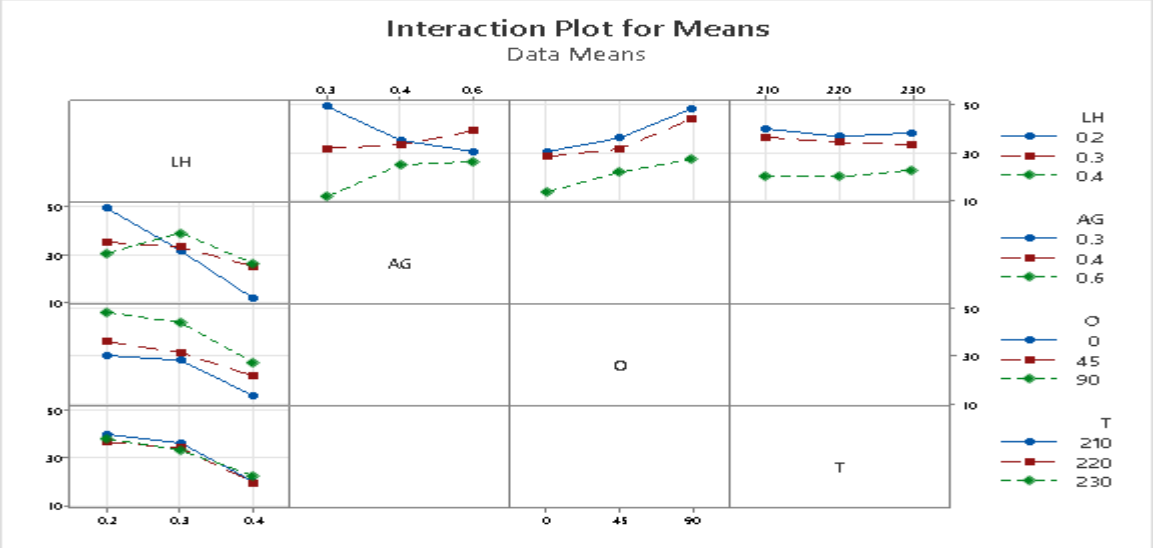

Figure 4: Mean effect plots TS Vs LH, AG, O, T, NN

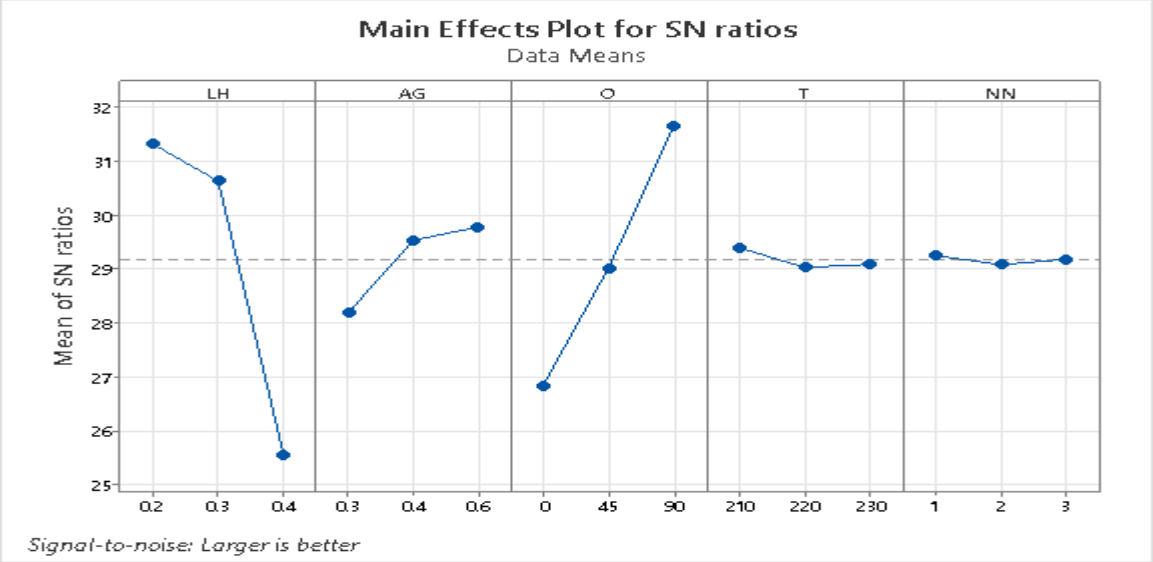

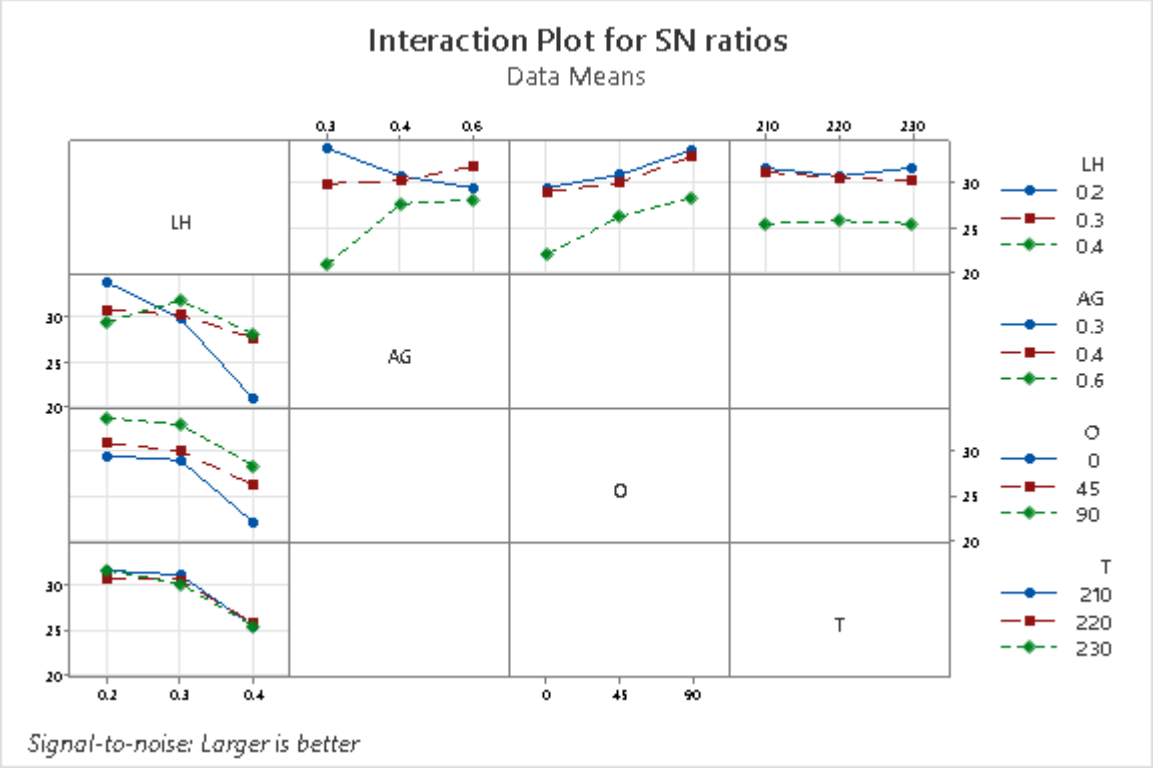

Figure 5: S/N ratios of TS Vs LH, AG, O, T, NN

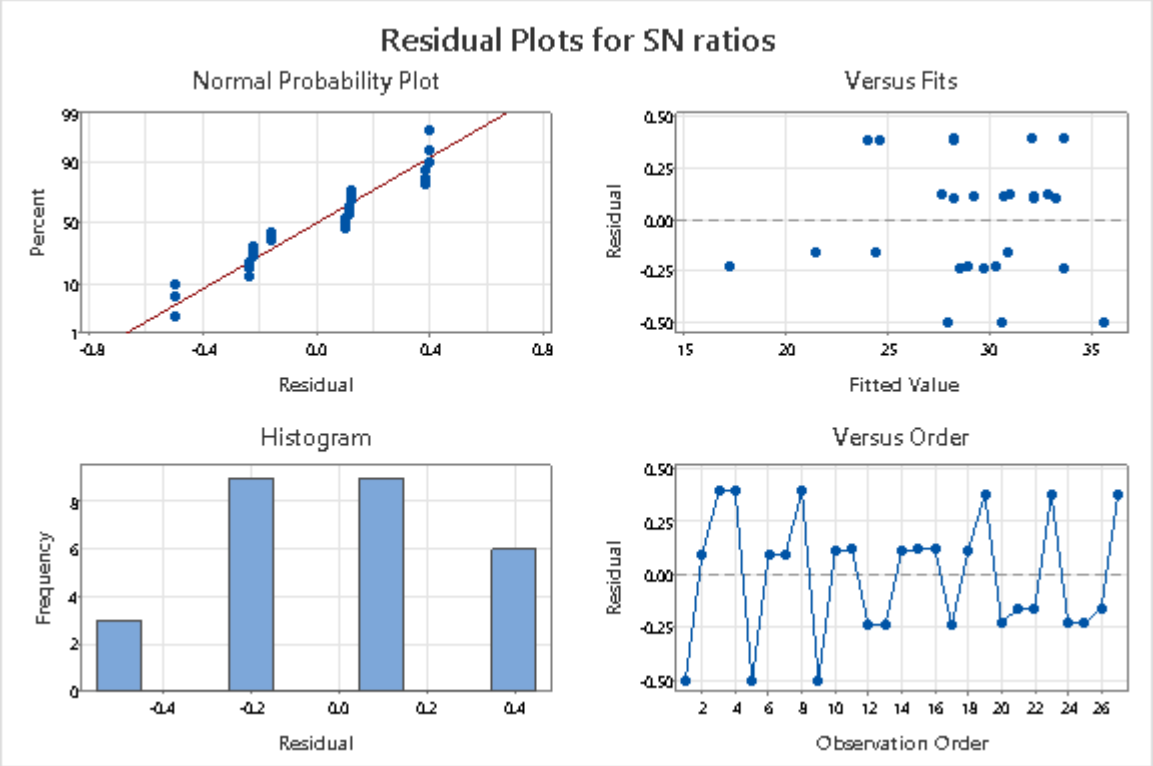

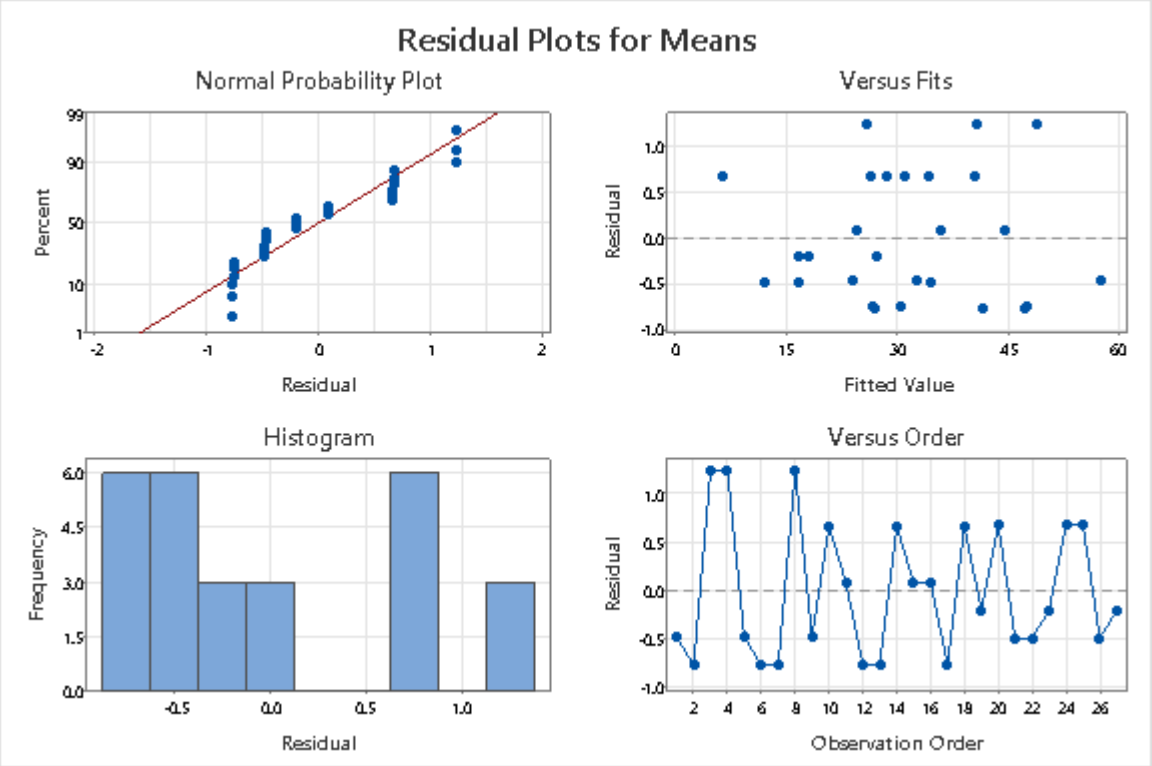

Figure 6: Residual Plots for TS Vs LH, AG, O, T, NN

Linear Model Analysis: SN ratios versus LH, AG, O, T, NN

Table 5: Estimated Model Coefficients for SN ratios

Term	Coef	SE Coef	T	P
Constant	29.1652	0.1416	205.992	0.000
LH 0.2	2.1494	0.2002	10.735	0.000
LH 0.3	1.4623	0.2002	7.303	0.002
AG 0.3	-0.9729	0.2002	-4.859	0.008
AG 0.4	0.3618	0.2002	1.807	0.145
O 0	-2.3290	0.2002	-11.632	0.000
O 45	-0.1532	0.2002	-0.765	0.487
T 210	0.2231	0.2002	1.114	0.328
T 220	-0.1386	0.2002	-0.692	0.527
NN 1	0.0777	0.2002	0.388	0.718
NN 2	-0.0875	0.2002	-0.437	0.685
LH*AG 0.2 0.3	3.4632	0.2832	12.230	0.000
LH*AG 0.2 0.4	-0.9532	0.2832	-3.366	0.028
LH*AG 0.3 0.3	0.2209	0.2832	0.780	0.479
LH*AG 0.3 0.4	-0.7806	0.2832	-2.757	0.051
LH*O 0.2 0	0.4549	0.2832	1.606	0.183
LH*O 0.2 45	-0.3112	0.2832	-1.099	0.334
LH*O 0.3 0	0.6860	0.2832	2.422	0.073
LH*O 0.3 45	-0.4841	0.2832	-1.710	0.163
LH*T 0.2 210	0.0616	0.2832	0.218	0.838
LH*T 0.2 220	-0.4507	0.2832	-1.592	0.187
LH*T 0.3 210	0.2778	0.2832	0.981	0.382
LH*T 0.3 220	0.0943	0.2832	0.333	0.756

Model Summary

S	R-Sq	R-Sq(adj)
0.7357	99.50%	96.74%

Table 6: Analysis of Variance for SN ratios

Source	DF	Seq SS	Adj SS	Adj MS	F	P
LH	2	178.229	178.229	89.1144	164.65	0.000
AG	2	13.059	13.059	6.5296	12.06	0.020
O	2	104.482	104.482	52.2411	96.52	0.000
T	2	0.685	0.685	0.3425	0.63	0.577
NN	2	0.124	0.124	0.0621	0.11	0.894
LH*AG	4	121.670	121.670	30.4176	56.20	0.001
LH*O	4	9.370	9.370	2.3426	4.33	0.092
LH*T	4	2.476	2.476	0.6190	1.14	0.450
Residual Error	4	2.165	2.165	0.5412		
Total	26	432.261				

Linear Model Analysis: Means versus LH, AG, O, T, NN

Table 7: Estimated Model Coefficients for Means

Term	Coef	SE Coef	T	P
Constant	31.4396	0.3377	93.105	0.000
LH 0.2	6.9937	0.4775	14.645	0.000
LH 0.3	3.3826	0.4775	7.083	0.002
AG 0.3	-0.4007	0.4775	-0.839	0.449
AG 0.4	-0.2185	0.4775	-0.458	0.671
O 0	-7.2019	0.4775	-15.081	0.000
O 45	-1.4796	0.4775	-3.098	0.036
T 210	0.8959	0.4775	1.876	0.134
T 220	-1.0174	0.4775	-2.130	0.100
NN 1	-0.3896	0.4775	-0.816	0.460
NN 2	0.2548	0.4775	0.534	0.622
LH*AG 0.2 0.3	11.4274	0.6754	16.921	0.000
LH*AG 0.2 0.4	-2.9381	0.6754	-4.351	0.012
LH*AG 0.3 0.3	-2.5215	0.6754	-3.734	0.020
LH*AG 0.3 0.4	-1.2770	0.6754	-1.891	0.132
LH*O 0.2 0	-0.7148	0.6754	-1.058	0.350
LH*O 0.2 45	-0.7270	0.6754	-1.077	0.342
LH*O 0.3 0	0.8563	0.6754	1.268	0.274
LH*O 0.3 45	-1.6093	0.6754	-2.383	0.076
LH*T 0.2 210	0.7774	0.6754	1.151	0.314
LH*T 0.2 220	-0.5959	0.6754	-0.882	0.427
LH*T 0.3 210	0.8019	0.6754	1.187	0.301
LH*T 0.3 220	0.6352	0.6754	0.941	0.400

Model Summary

S	R-Sq	R-Sq(adj)
1.7546	99.68%	97.92%

Table 8: Analysis of Variance for Means

Source	DF	Seq SS	Adj SS	Adj MS	F	P
LH	2	1512.19	1512.19	756.096	245.59	0.000
AG	2	5.33	5.33	2.663	0.87	0.487
O	2	1164.82	1164.82	582.408	189.17	0.000
T	2	16.67	16.67	8.337	2.71	0.180
NN	2	2.11	2.11	1.057	0.34	0.728

LH*AG	4	1058.37	1058.37	264.592	85.94	0.000
LH*O	4	51.91	51.91	12.978	4.22	0.096
LH*T	4	27.66	27.66	6.914	2.25	0.226
Residual Error	4	12.31	12.31	3.079		
Total	26	3851.38				

Table 9: Response Table for Signal to Noise Ratios

Larger is better

Level	LH	AG	O	T	NN
1	31.31	28.19	26.84	29.39	29.24
2	30.63	29.53	29.01	29.03	29.08
3	25.55	29.78	31.65	29.08	29.18
Delta	5.76	1.58	4.81	0.36	0.17
Rank	1	3	2	4	5

Table 10: Response Table for Means

Level	LH	AG	O	T	NN
1	38.43	31.04	24.24	32.34	31.05
2	34.82	31.22	29.96	30.42	31.69
3	21.06	32.06	40.12	31.56	31.57
Delta	17.37	1.02	15.88	1.91	0.64
Rank	1	4	2	3	5

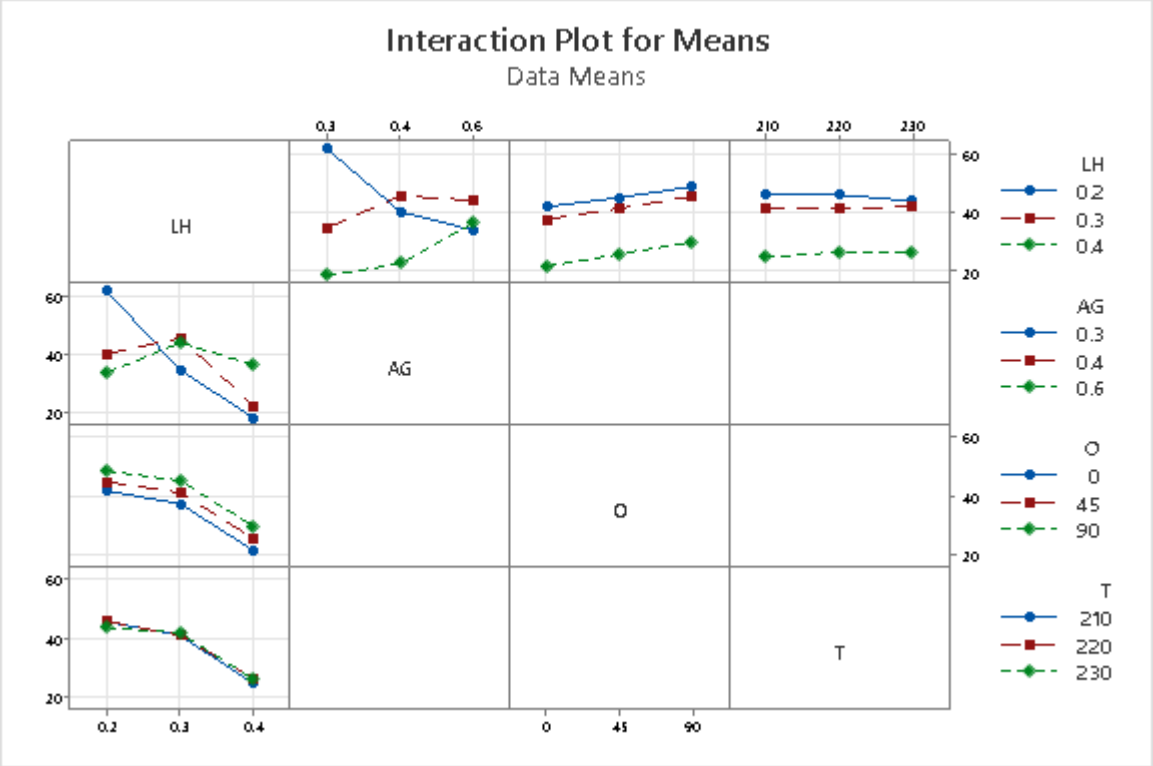

Figure 7: Mean effect plots FS Vs LH, AG, O, T, NN

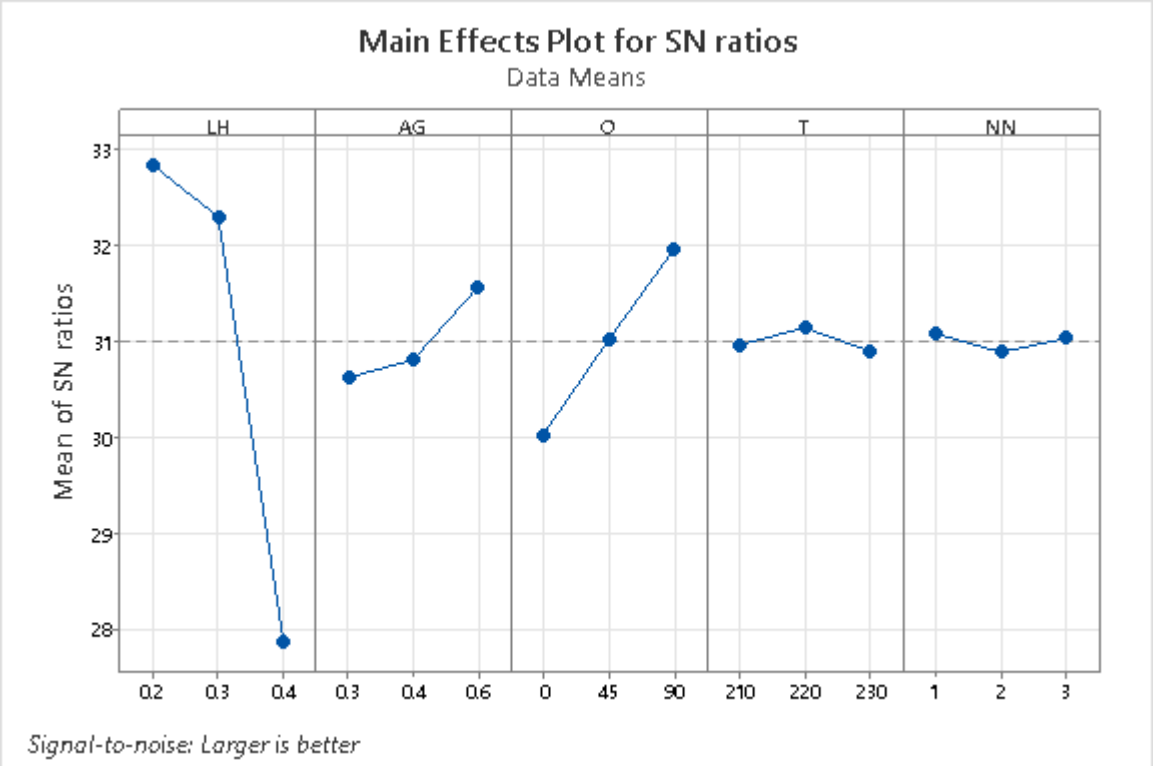

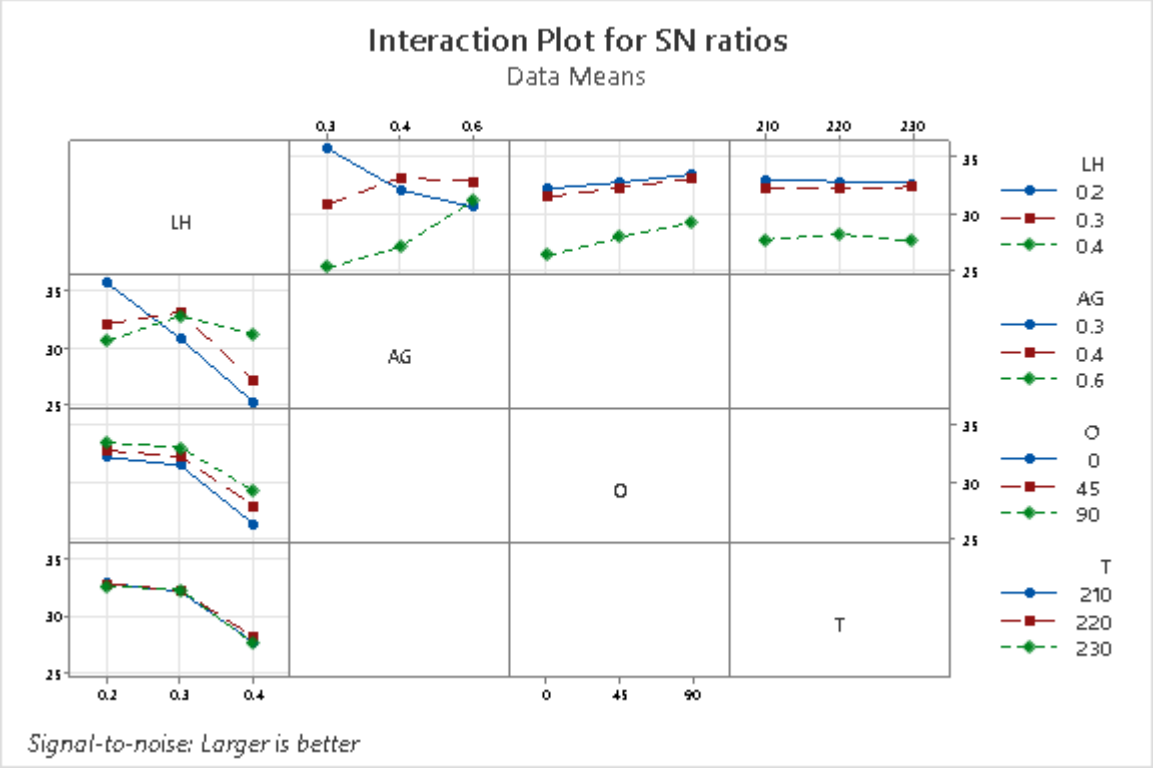

Figure 8: S/N ratios of FS Vs LH, AG, O, T, NN

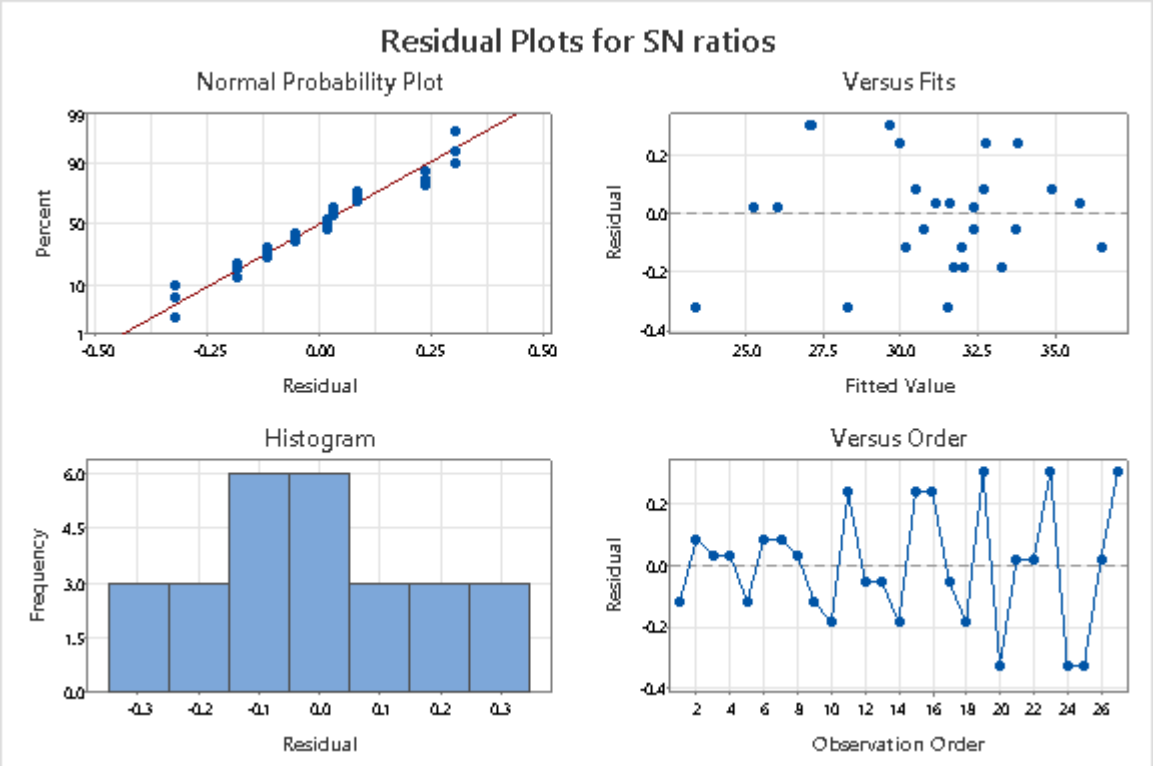

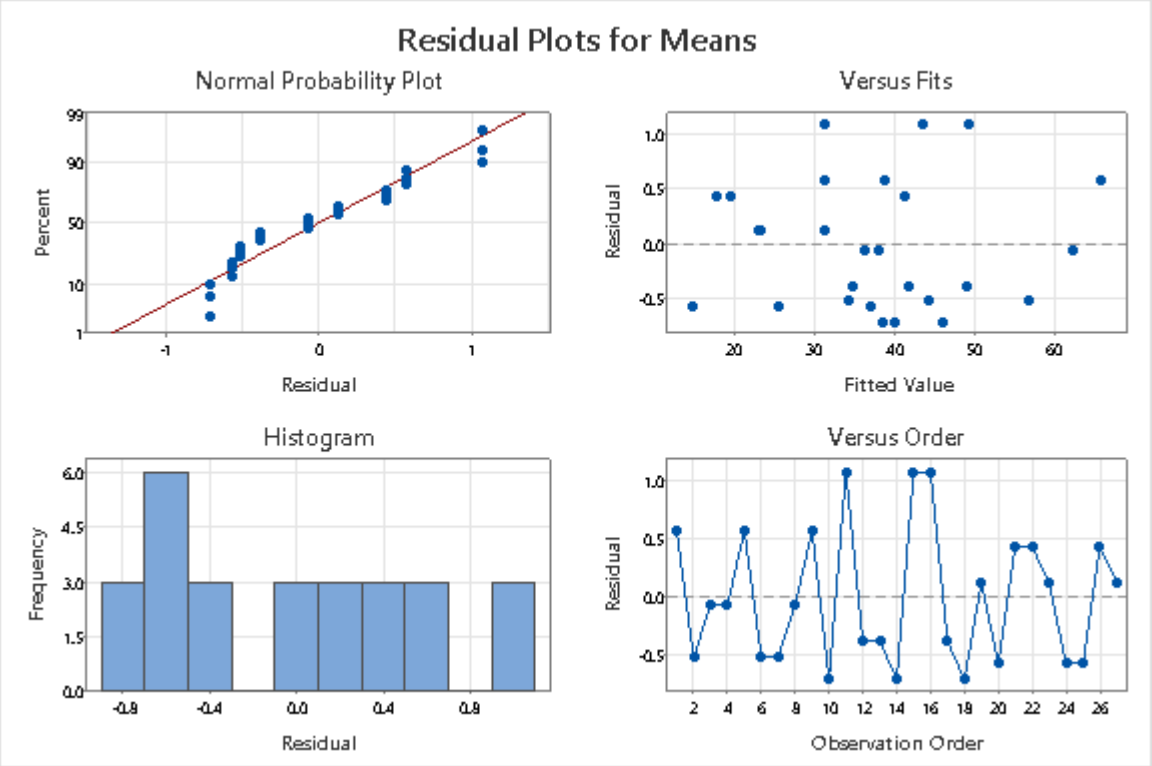

Figure 9: Residual Plots for FS Vs LH, AG, O, T, NN

Linear Model Analysis: SN ratios versus LH, AG, O, T, NN

Table 11: Estimated Model Coefficients for SN ratios

Term	Coef	SE Coef	T	P
Constant	30.9956	0.09307	333.034	0.000
LH 0.2	1.8404	0.13162	13.983	0.000
LH 0.3	1.2996	0.13162	9.874	0.001
AG 0.3	-0.3766	0.13162	-2.861	0.046
AG 0.4	-0.1920	0.13162	-1.459	0.218
O 0	-0.9750	0.13162	-7.407	0.002
O 45	0.0141	0.13162	0.107	0.920
T 210	-0.0378	0.13162	-0.287	0.788
T 220	0.1422	0.13162	1.080	0.341
NN 1	0.0819	0.13162	0.622	0.568
NN 2	-0.1149	0.13162	-0.873	0.432
LH*AG 0.2 0.3	3.3233	0.18614	17.854	0.000
LH*AG 0.2 0.4	-0.5314	0.18614	-2.855	0.046
LH*AG 0.3 0.3	-1.0789	0.18614	-5.796	0.004
LH*AG 0.3 0.4	1.0743	0.18614	5.771	0.004
LH*O 0.2 0	0.3687	0.18614	1.981	0.119
LH*O 0.2 45	-0.0649	0.18614	-0.349	0.745
LH*O 0.3 0	0.1692	0.18614	0.909	0.415
LH*O 0.3 45	-0.0135	0.18614	-0.073	0.946
LH*T 0.2 210	0.1295	0.18614	0.696	0.525
LH*T 0.2 220	-0.0960	0.18614	-0.516	0.633
LH*T 0.3 210	-0.0364	0.18614	-0.195	0.855
LH*T 0.3 220	-0.1435	0.18614	-0.771	0.484

Model Summary

S	R-Sq	R-Sq(adj)
0.4836	99.65%	97.69%

Table 12: Analysis of Variance for SN ratios

Source	DF	Seq SS	Adj SS	Adj MS	F	P
LH	2	134.423	134.423	67.2117	287.38	0.000
AG	2	4.519	4.519	2.2593	9.66	0.029
O	2	16.866	16.866	8.4332	36.06	0.003
T	2	0.293	0.293	0.1464	0.63	0.580
NN	2	0.189	0.189	0.0944	0.40	0.692
LH*AG	4	103.620	103.620	25.9049	110.76	0.000
LH*O	4	2.376	2.376	0.5941	2.54	0.194
LH*T	4	0.507	0.507	0.1266	0.54	0.717
Residual Error	4	0.936	0.936	0.2339		
Total	26	263.728				

Linear Model Analysis: Means versus LH, AG, O, T, NN

Table 13: Estimated Model Coefficients for Means

Term	Coef	SE Coef	T	P
Constant	37.6581	0.2849	132.164	0.000
LH 0.2	7.6974	0.4030	19.102	0.000
LH 0.3	3.9407	0.4030	9.780	0.001
AG 0.3	0.7552	0.4030	1.874	0.134
AG 0.4	-1.3470	0.4030	-3.343	0.029
O 0	-3.7537	0.4030	-9.315	0.001
O 45	-0.0981	0.4030	-0.244	0.820
T 210	-0.2359	0.4030	-0.585	0.590
T 220	0.3685	0.4030	0.915	0.412
NN 1	-0.0637	0.4030	-0.158	0.882
NN 2	-0.2104	0.4030	-0.522	0.629
LH*AG 0.2 0.3	15.5693	0.5699	27.321	0.000
LH*AG 0.2 0.4	-3.6052	0.5699	-6.326	0.003
LH*AG 0.3 0.3	-7.4541	0.5699	-13.080	0.000
LH*AG 0.3 0.4	5.4815	0.5699	9.619	0.001
LH*O 0.2 0	0.4781	0.5699	0.839	0.449
LH*O 0.2 45	-0.1241	0.5699	-0.218	0.838
LH*O 0.3 0	-0.1052	0.5699	-0.185	0.863
LH*O 0.3 45	0.0093	0.5699	0.016	0.988
LH*T 0.2 210	0.8670	0.5699	1.521	0.203
LH*T 0.2 220	0.3926	0.5699	0.689	0.529
LH*T 0.3 210	-0.0130	0.5699	-0.023	0.983
LH*T 0.3 220	-0.6907	0.5699	-1.212	0.292

Model Summary

S	R-Sq	R-Sq(adj)
1.4806	99.79%	98.64%

Table 14: Analysis of Variance for Means

Source	DF	Seq SS	Adj SS	Adj MS	F	P
LH	2	1892.03	1892.03	946.017	431.57	0.000
AG	2	24.62	24.62	12.308	5.61	0.069
O	2	260.43	260.43	130.215	59.40	0.001
T	2	1.88	1.88	0.941	0.43	0.678
NN	2	1.11	1.11	0.555	0.25	0.788

LH*AG	4	1971.74	1971.74	492.934	224.87	0.000
LH*O	4	1.83	1.83	0.456	0.21	0.921
LH*T	4	13.78	13.78	3.444	1.57	0.336
Residual Error	4	8.77	8.77	2.192		
Total	26	4176.18				

Table 15: Response Table for Signal to Noise Ratios

Larger is better

Level	LH	AG	O	T	NN
1	32.84	30.62	30.02	30.96	31.08
2	32.30	30.80	31.01	31.14	30.88
3	27.86	31.56	31.96	30.89	31.03
Delta	4.98	0.95	1.94	0.25	0.20
Rank	1	3	2	4	5

Table 16: Response Table for Means

Level	LH	AG	O	T	NN
1	45.36	38.41	33.90	37.42	37.59
2	41.60	36.31	37.56	38.03	37.45
3	26.02	38.25	41.51	37.53	37.93
Delta	19.34	2.10	7.61	0.60	0.48
Rank	1	3	2	4	5

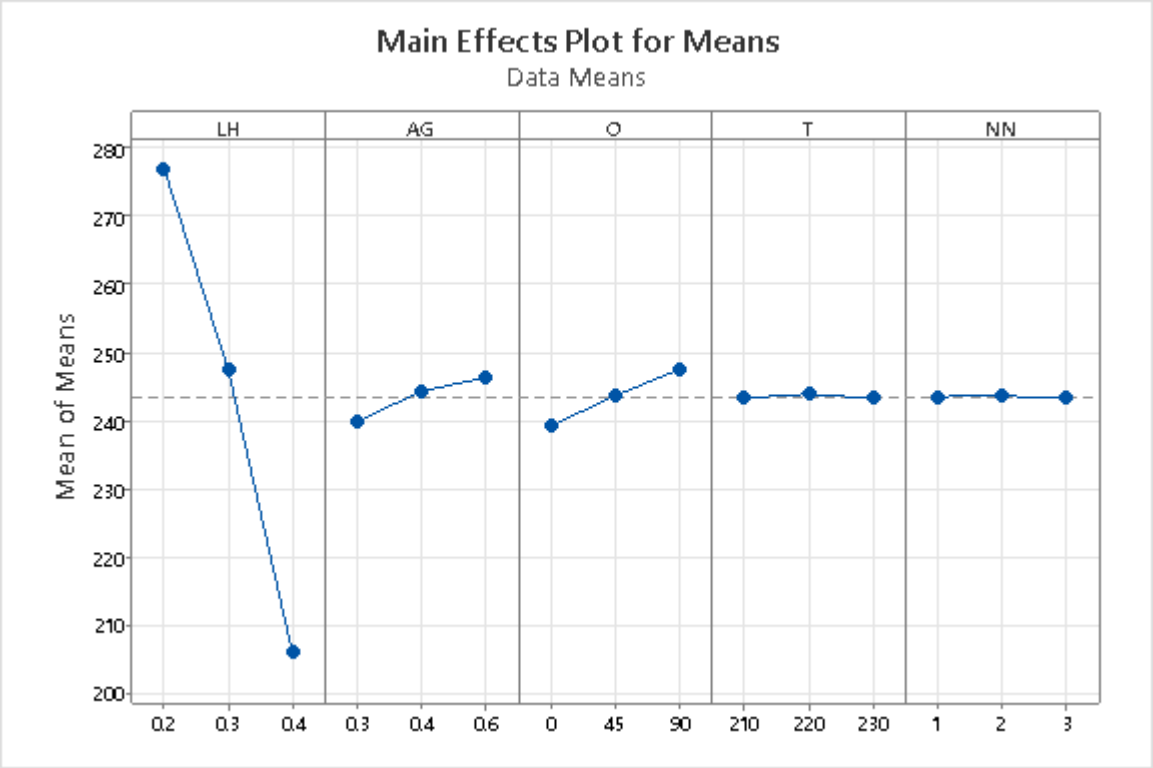

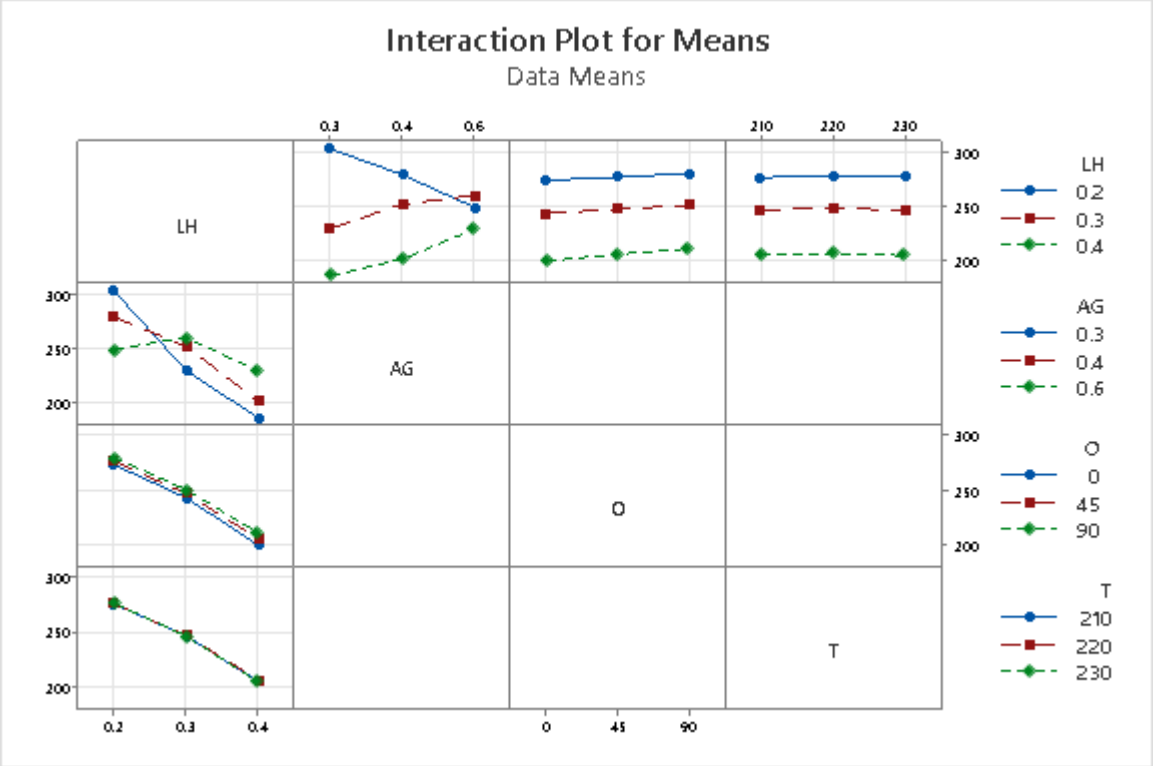

Figure 10: Mean effect plots IS Vs LH, AG, O, T, NN

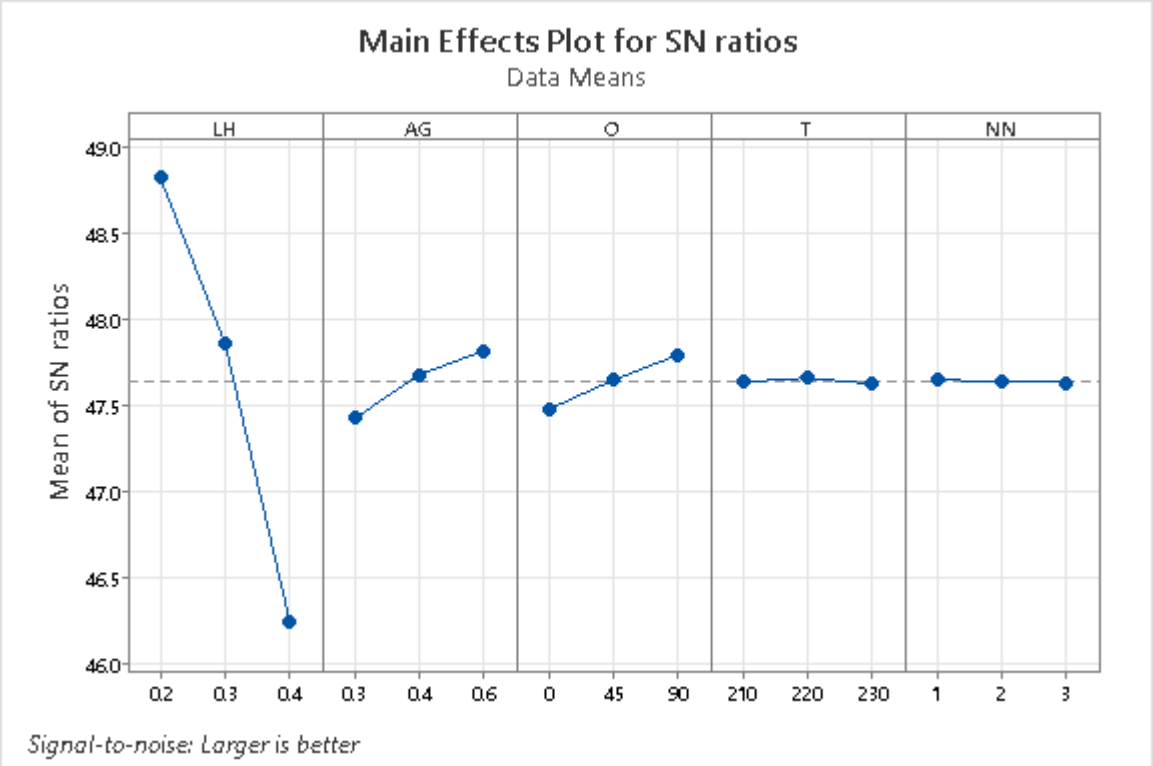

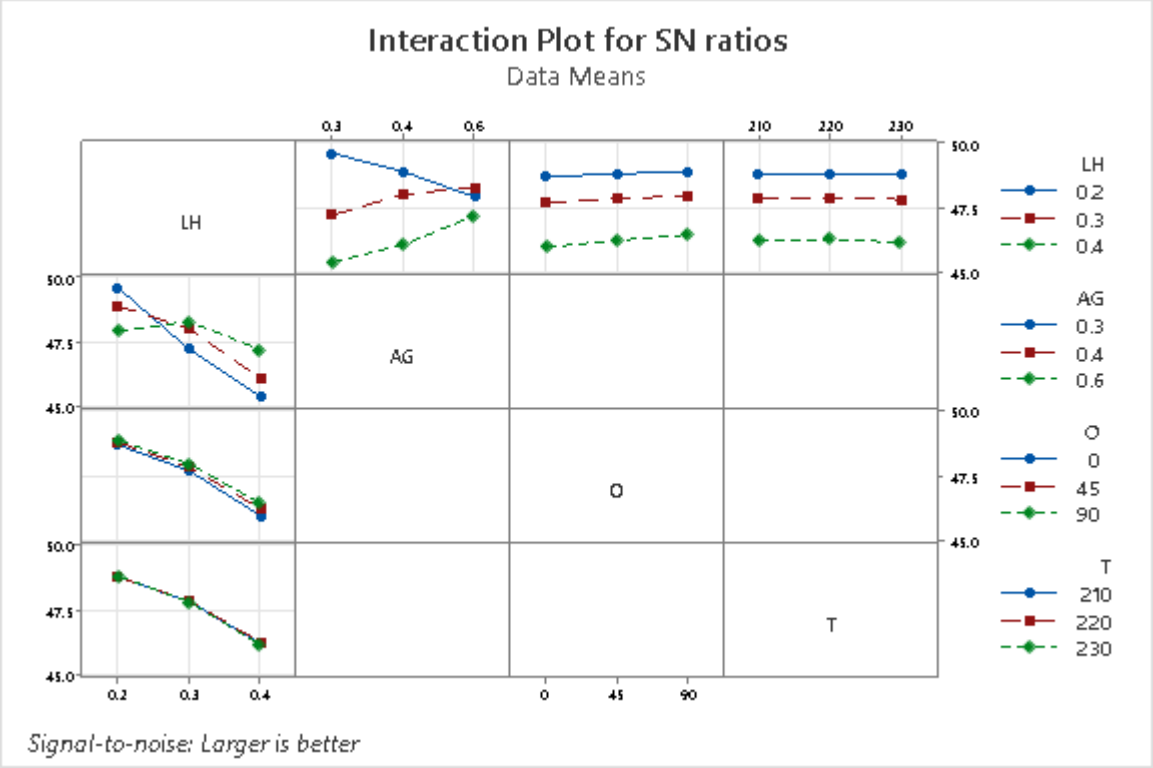

Figure 11: S/N ratios of IS Vs LH, AG, O, T, NN

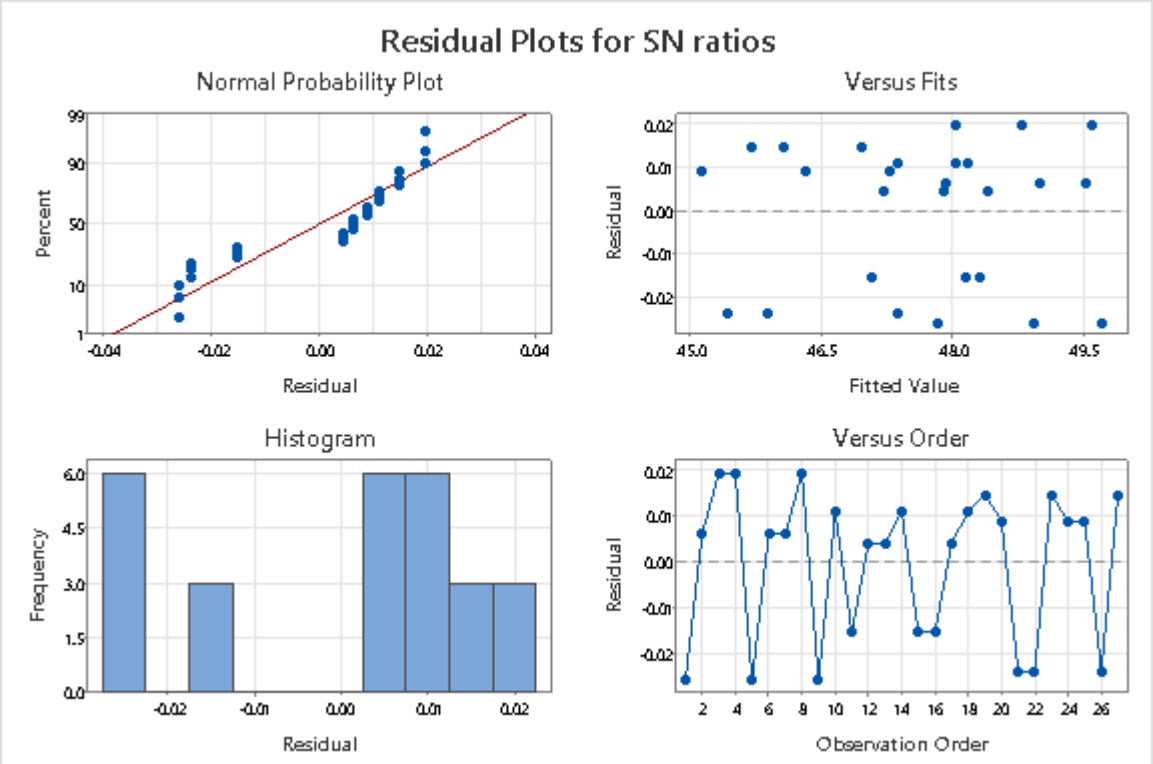

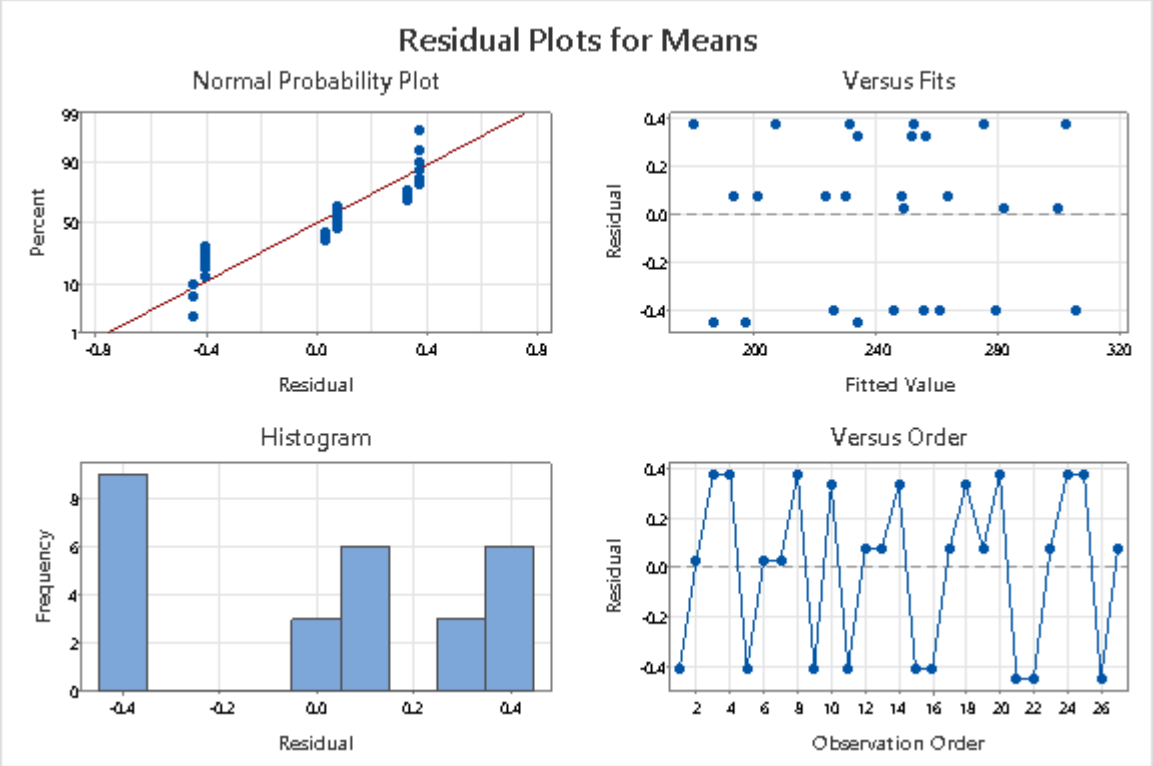

Figure 12: Residual Plots for IS Vs LH, AG, O, T, NN

Linear Model Analysis: SN ratios versus LH, AG, O, T, NN

Table 17: Estimated Model Coefficients for SN ratios

Term	Coef	SE Coef	T	P
Constant	47.6413	0.008059	5911.443	0.000
LH 0.2	1.1805	0.011397	103.574	0.000
LH 0.3	0.2165	0.011397	18.993	0.000
AG 0.3	-0.2160	0.011397	-18.956	0.000
AG 0.4	0.0396	0.011397	3.472	0.026
O 0	-0.1614	0.011397	-14.159	0.000
O 45	0.0069	0.011397	0.609	0.576
T 210	-0.0045	0.011397	-0.392	0.715
T 220	0.0201	0.011397	1.760	0.153
NN 1	0.0076	0.011397	0.663	0.544
NN 2	0.0002	0.011397	0.017	0.987
LH*AG 0.2 0.3	1.0152	0.016118	62.987	0.000
LH*AG 0.2 0.4	0.0504	0.016118	3.126	0.035
LH*AG 0.3 0.3	-0.4095	0.016118	-25.403	0.000
LH*AG 0.3 0.4	0.1358	0.016118	8.428	0.001
LH*O 0.2 0	0.0611	0.016118	3.791	0.019
LH*O 0.2 45	-0.0065	0.016118	-0.401	0.709
LH*O 0.3 0	0.0278	0.016118	1.723	0.160
LH*O 0.3 45	-0.0040	0.016118	-0.251	0.814
LH*T 0.2 210	-0.0086	0.016118	-0.531	0.623
LH*T 0.2 220	-0.0252	0.016118	-1.562	0.193
LH*T 0.3 210	0.0035	0.016118	0.218	0.838
LH*T 0.3 220	-0.0062	0.016118	-0.384	0.720

Model Summary

S	R-Sq	R-Sq(adj)
0.0419	99.98%	99.89%

Table 18: Analysis of Variance for SN ratios

Source	DF	Seq SS	Adj SS	Adj MS	F	P
LH	2	30.5266	30.5266	15.2633	8703.70	0.000
AG	2	0.7145	0.7145	0.3572	203.71	0.000
O	2	0.4495	0.4495	0.2247	128.15	0.000
T	2	0.0060	0.0060	0.0030	1.71	0.291
NN	2	0.0011	0.0011	0.0005	0.30	0.756
LH*AG	4	10.3763	10.3763	2.5941	1479.24	0.000
LH*O	4	0.0668	0.0668	0.0167	9.52	0.025
LH*T	4	0.0127	0.0127	0.0032	1.81	0.289
Residual Error	4	0.0070	0.0070	0.0018		
Total	26	42.1603				

Linear Model Analysis: Means versus LH, AG, O, T, NN

Table 19: Estimated Model Coefficients for Means

Term	Coef	SE Coef	T	P
Constant	243.496	0.1605	1517.281	0.000
LH 0.2	33.504	0.2270	147.622	0.000
LH 0.3	3.970	0.2270	17.494	0.000
AG 0.3	-3.674	0.2270	-16.189	0.000
AG 0.4	0.837	0.2270	3.688	0.021
O 0	-4.252	0.2270	-18.734	0.000
O 45	0.170	0.2270	0.751	0.495
T 210	-0.185	0.2270	-0.816	0.460
T 220	0.426	0.2270	1.877	0.134
NN 1	0.037	0.2270	0.163	0.878
NN 2	0.104	0.2270	0.457	0.671
LH*AG 0.2 0.3	29.407	0.3210	91.622	0.000
LH*AG 0.2 0.4	1.163	0.3210	3.623	0.022
LH*AG 0.3 0.3	-13.826	0.3210	-43.076	0.000
LH*AG 0.3 0.4	3.863	0.3210	12.036	0.000
LH*O 0.2 0	1.119	0.3210	3.485	0.025
LH*O 0.2 45	-0.170	0.3210	-0.531	0.624
LH*O 0.3 0	0.485	0.3210	1.512	0.205
LH*O 0.3 45	-0.104	0.3210	-0.323	0.763
LH*T 0.2 210	-0.081	0.3210	-0.254	0.812
LH*T 0.2 220	-0.526	0.3210	-1.639	0.177
LH*T 0.3 210	0.119	0.3210	0.369	0.731
LH*T 0.3 220	-0.159	0.3210	-0.496	0.646

Model Summary

S	R-Sq	R-Sq(adj)
0.8339	99.99%	99.94%

Table 20: Analysis of Variance for Means

Source	DF	Seq SS	Adj SS	Adj MS	F	P
LH	2	22883.1	22883.1	11441.6	16453.90	0.000
AG	2	200.2	200.2	100.1	143.98	0.000
O	2	312.9	312.9	156.4	224.98	0.000
T	2	2.5	2.5	1.2	1.77	0.281
NN	2	0.3	0.3	0.1	0.21	0.821

LH*AG	4	8396.2	8396.2	2099.1	3018.62	0.000
LH*O	4	21.0	21.0	5.2	7.53	0.038
LH*T	4	4.8	4.8	1.2	1.71	0.308
Residual Error	4	2.8	2.8	0.7		
Total	26	31823.7				

Table 21: Response Table for Signal to Noise Ratios

Larger is better

Level	LH	AG	O	T	NN
1	48.82	47.43	47.48	47.64	47.65
2	47.86	47.68	47.65	47.66	47.64
3	46.24	47.82	47.80	47.63	47.63
Delta	2.58	0.39	0.32	0.04	0.02
Rank	1	2	3	4	5

Table 22: Response Table for Means

Level	LH	AG	O	T	NN
1	277.0	239.8	239.2	243.3	243.5
2	247.5	244.3	243.7	243.9	243.6
3	206.0	246.3	247.6	243.3	243.4
Delta	71.0	6.5	8.3	0.7	0.2
Rank	1	3	2	4	5

The “larger-the-better” criterion was employed in this study to identify the optimal printing conditions that maximize mechanical performance. Under this criterion, higher S/N ratios indicate superior quality and stability of the printed components. Based on the Taguchi optimization framework, the optimal combination of process parameters identified from Table 2 was determined to be: orientation (OR) at Level 3 (90°), layer height (LH) at 0.2 mm, printing temperature (Temp) at 220°C, and nozzle material (TiC) at Level 3. This parameter configuration yielded the highest overall mechanical performance in terms of strength and impact resistance [13]. Furthermore, the influence and statistical significance of each process parameter on impact strength were analyzed using Analysis of Variance (ANOVA). The ANOVA results for all mechanical properties are presented in Table 4. Parameters with p-values less than 0.05 were considered statistically significant, indicating a strong influence on the corresponding mechanical property. Among the evaluated parameters, layer height (LH) exhibited the most significant effect on mechanical performance. Parameters with p-values greater than 0.05 were deemed to have an insignificant impact on the response variables. The relative effects of the five process parameters on the mechanical properties, particularly on

mean impact strength, are illustrated in Figure 4, derived from the experimental dataset [14]. Figure 4-12 illustrates the influence of various process parameters on the mechanical properties of carbon fiber-reinforced PLAPRO (CFRP) composites, indicating the combinations that yielded the highest and lowest experimental responses. The signal-to-noise (S/N) ratios for each mechanical property were computed based on Taguchi's optimization method to identify the most influential process settings. The optimized parameter configurations for tensile strength (TS), flexural strength (FS), impact strength (IM) are summarized below. Significant effects of printing parameters and composite characteristics on mechanical performance were observed. The optimal FDM printing conditions corresponding to the highest measured mechanical values as shown in Figures 4-12 were a layer height of 0.2 mm, air gap of 0.4 mm, printing temperature of 220°C, and titanium carbide (TiC) nozzle. Under these optimized conditions, the composite achieved an impact strength of 480 J/m, flexural strength of 70 MPa, As reported in previous studies, the incorporation of PLA-PRO fibers and carbon fibers has been shown to significantly enhance the mechanical properties of polymer composites [15]. The results obtained in this investigation are consistent with prior research, confirming that 20 wt% carbon fiber reinforcement substantially improves the mechanical performance of PLA-PRO based composites. However, excessive fiber loading may adversely affect the processability of the material, leading to increased porosity and reduced interfacial bonding, which ultimately diminish mechanical performance.

According to Table 5-22, variations in experimental conditions particularly differences in printing orientation (OR) contributed to discrepancies in optimal mechanical values among samples. The results indicated that flexural strength improved with higher layer height (LH), printing temperature (Temp), and the use of a TiC nozzle, while tensile and impact strengths exhibited a positive correlation with increased printing temperature and orientation angle. Overall, these findings reinforce that carbon fiber reinforcement in PLA composites enhances stiffness and strength while maintaining lightweight characteristics. Nonetheless, an optimal balance between fiber content and processability must be achieved. Further research is recommended to systematically evaluate this trade-off and ensure that the mechanical benefits of fiber reinforcement outweigh potential processing limitations [16]. In Fused Deposition Modelling (FDM), the layer height is a critical parameter influencing both the mechanical performance and surface quality of printed components. As illustrated in Figure 4-6, **a** layer height of 0.2 mm resulted in superior structural integrity compared to 0.3 mm and 0.4 mm, reducing porosity and promoting effective interlayer adhesion. Optimized layer height ensures

proper filling of voids within the printed structure, leading to enhanced strength and improved surface finish [17]. Mechanical evaluation of the specimens was performed using the Izod impact test**,** wherein a hammer strikes the notched sample to determine impact resistance. The results indicated anisotropic behavior, with higher impact strength observed along the fiber alignment direction and reduced strength in the transverse direction, reflecting the directional dependency of mechanical performance in fiber-reinforced PLA composites [18].

At a 45° printing orientation, the specimens exhibited moderate mechanical strength. Printing temperature was identified as a critical factor influencing both the mechanical performance and surface quality of 3D-printed components. Maintaining optimal temperature is essential to ensure proper interlayer adhesion through conduction and convection heat transfer mechanisms**,** thereby maximizing structural integrity and achieving a smooth surface finish. At a lower temperature of 200 °C, increased porosity was observed, whereas at 220 °C**,** porosity decreased significantly. This improvement is attributed to enhanced interlayer bonding at higher temperatures, which promotes stronger adhesion between deposited layers and results in improved mechanical strength and surface quality.

To sum up, the overall efficacy, durability, and quality of 3D printed products in FDM are greatly affected by essential parameters such as layer height, material qualities, temperature control, infill density, and others. By thoroughly understanding and refining these aspects, designers and manufacturers may improve the printed products used in the medical and aerospace industries, making them more reliable and useful while still meeting all the necessary standards.

4 Conclusions

- The study investigated the amalgamation of carbon fiber with various polymers in additive manufacturing processes utilizing 3D printing technology. It highlighted the promise of carbon fiber and its varied applications across multiple sectors. The layer-by-layer fabrication approach via fused deposition modeling facilitates the swift production of intricate designs, with the quality of the resultant components influenced by particular printing parameters and the precise type of carbon fiber reinforced PLA utilized. The versatility of carbon fiber, together with its extensive applications across several industries, underscores its significance. Furthermore, the recyclability of carbon fiber reinforced PLA offers supplementary advantages for potential applications.

- A composite material made of carbon fiber-reinforced Polylactic Acid (PLA-PRO) was successfully 3D printed utilizing the Fused Deposition Modeling (FDM)process with the L_{27} orthogonal array. The purpose of this study was to evaluate the printed material's tensile and flexural strengths. In order to assess the results and find the best process parameters for the printing technique, the study used the Taguchi methodology.
- The results showed that the TiC_4 nozzle, LH-0.2 mm, OR-90^0, Temp-220^0C, an air gap of 0.4 mm, and these particular conditions produced the highest values for Tensile Strength and Flexural Strength, with 61 MPa and 70 MPa, respectively, and an impact strength of 480 J/M. The strength improvement was mostly due to these characteristics, which showed a 30% improvement over values reported in previous research on carbon fiber reinforcing with PLA. Also, compared to PLA alone, study shows that carbon fiber-reinforced PLA has a significant improvement in characteristics of 30–40%.
- Enhanced mechanical properties of high-performance PLA composites have been achieved through the integration of Taguchi optimization, carbon fiber reinforcing, and the Fused Deposition Modeling (FDM) technique. Our understanding of additive manufacturing and composite materials has grown thanks to this study's findings. Researchers and engineers working to enhance the mechanical properties of polymer composites for uses in fields as diverse as dentistry and automobiles can also benefit greatly from their findings. The relentless quest for new materials is pushing the industry even farther studies in this area, providing opportunities for the creation of high-tech composites that exhibit remarkable characteristics. As a result, recycled carbon fiber and carbon fiber reinforced polymer composites open up new avenues for engineering applications across a wide range of industries.

Conflicts of Interest

The authors declare that there are no conflicts of interest regarding the publication of this paper.

References

1. Jayakrishna, M., Vijay, M., Khan, B.: An overview of extensive analysis of 3DPrinting Applications in the Manufacturing Sector.J. Eng. **2023**, 1–23 (2023)
2. Iftekar, S.F., Aabid, A., Amir, A., Baig, M.: Advancements and limitations in 3D Printing materials and technologies: A critical review. Polym. (Basel), **15**, 11, (2023)
3. Huang, H., Liu, W., Liu, Z.: Additive manufacturing-inspired approach to re-manufacture fiber reinforced plastic with programmable orientation of recycled carbon fiber. Compos. Commun. **38**, 101521 (Feb. 2023)
4. Ateeq, M., Shafique, M., Azam, A., Rafiq, M.: A review of 3D printing of the recycled

carbon fiber reinforced polyme composites: Processing, potential, and perspectives, *J.Mater.Res. Tech- nol*, vol. 26, pp. 2291–2309, Sep. (2023)
5. Ceylan, İ., Çakıcı, N., Alp, Aytaç, A.: Sustainable 3D printing with alkali-treated hemp fiber-reinforced polycarbonate composites. Cellulose. **31**(7), 4477–4495 (2024)
6. Mahmood, A., Perveen, F., Chen, S., Akram, T., Irfan, A.: Polymer Composites in 3D/4D Printing: Materials, Advances, and Prospects. Molecules vol.29, no.319.pp.1–32, 2024
7. Pezzana, L., Wolff, R., Stampfl, J., Liska, R., Sangermano, M.: High temperature vat photopolymerization 3D printing of fully bio-based composites: Green vegetable oil epoxy matrix & bio- derived filler powder, *Addit. Manuf*, vol. 79, Jan. (2024)
8. Marabello, G., Borsellino, C., Bella, G.D.: Carbon Fiber 3D Printing: Technologies and Performance A brief review. Mater. (Basel),**16**, 23, (2023)
9. Lopes, B.J., Roberto, J., Almeida, M.: Science Direct Initial development and characterization of carbon fiber reinforced ABS for future Additive Manufacturing applications, *Mater. Today Proc*, vol. 8, pp. 719–730, (2019)
10. Rabinowitz, A., DeSantis, P.M., Basgul, C., Spece, H., Kurtz, S.M.: Taguchi optimization of 3D printed short carbon fiber polyether ketone ketone (CFR PEKK). J. Mech. Behav. Biomed. Mater. **145**, p105981 (Sep. 2023)
11. Lokesh, N., Praveena, B.A., Sudheer Reddy, J., Vasu, V.K., Vijaykumar, S.: Evaluation on effect of printing process parameter through Taguchi approach on mechanical properties of 3D printed PLA specimens using FDM at constant printing temperature. Mater. Today Proc. **52**, 1288–1293 (2022)
12. Park, J.W., Shin, J.H., Shim, G.S., Sim, K.B., Jang, S.W., Kim, H.J.: Mechanical strength enhancement of polylactic acid hybrid composites. Polym. (Basel).**11**(2),1–12 (2019)
13. Kam, M., Ipekçi, A., Şengül: Taguchi optimization off used deposition modeling process parameters on mechanical characteristics of PLA + lament material. Sci. Iran. **29**(1), 79–89 (2022)
14. Hikmat, M., Rostam, S., Ahmed, Y.M.: Investigation of tensile property-based Taguchi method of PLA parts fabricated by FDM 3D printing technology. Results Eng. **11**, 100264 (2021)
15. Parandoush, P, P., Lin, D.: A, D.: A.: A review on additive manufacturing of polymer-fiber composites. Compos. Struct.**182**,36–53(2017)
16. Sharma, K., Kumar, K., Singh, K.R., Rawat, M.S.: Optimization of FDM 3D printing process parameters using Taguchi technique. IOP Conf. Ser. Mater. Sci. Eng. **1168**(1), 012022 (2021)
17. Chohan, J.S., et al.: Optimization of FDM Printing process parameters on Surface Finish, Thickness, and outer dimension with ABS polymer specimens using Taguchi Orthogonal array and genetic algorithms. Math. Probl. Eng. **2022**, 1–13 (2022)
18. Vishal, K., Rajkumar, K., Sabarinathan, P., Dhinakaran, V.: Mechanical and wear characteristics investigation on 3D printed Silicon filled poly (lactic acid) Bio polymer Composite fabricated by fused deposition modeling. Silicon, no. 0123456789, (2022)
19. Yavas, D., Zhang, Z., Liu, Q., Wu, D.: Fracture behavior of 3D printed carbon fiber-reinforced polymer composites, *Compos. Sci. Technol*, vol. 208, no. June p. 108741, 2021. (2020)
20. Van De Werken, N., Tekin alp, H., Khanbalik, P., Ozcan, S.: Additively manufactured carbon fiber-reinforced composites: State of the art and perspective, *Addit. Manuf*, vol.31, no. July p.100962, 2020. (2019)